

**NUCLEAR DATA AND MEASUREMENTS SERIES**

**ANL/NDM-44**

**The Interaction of Fast Neutrons with  $^{60}\text{Ni}$**

by

A. Smith, P. Guenther, D. Smith, and J. Whalen

January 1979

**ARGONNE NATIONAL LABORATORY,  
ARGONNE, ILLINOIS 60439, U.S.A.**

# NUCLEAR DATA AND MEASUREMENTS SERIES

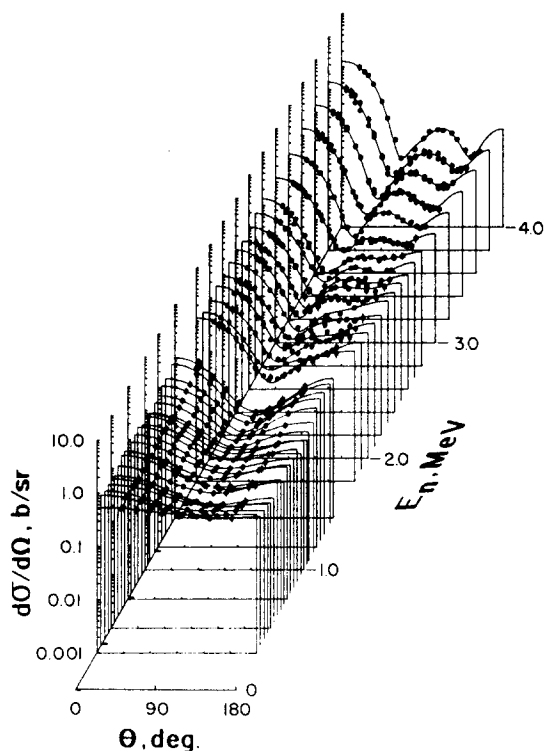
ANL/NDM-44

THE INTERACTION OF FAST NEUTRONS WITH  $^{60}\text{Ni}^*$

by

A. Smith, P. Guenther,  
D. Smith and J. Whalen

January 1979



U of C-AUA-USDOE

ARGONNE NATIONAL LABORATORY,  
ARGONNE, ILLINOIS 60439, U.S.A.

The facilities of Argonne National Laboratory are owned by the United States Government. Under the terms of a contract (W-31-109-Eng-38) between the U. S. Department of Energy, Argonne Universities Association and The University of Chicago, the University employs the staff and operates the Laboratory in accordance with policies and programs formulated, approved and reviewed by the Association.

#### MEMBERS OF ARGONNE UNIVERSITIES ASSOCIATION

The University of Arizona	Kansas State University	The Ohio State University
Carnegie-Mellon University	The University of Kansas	Ohio University
Case Western Reserve University	Loyola University	The Pennsylvania State University
The University of Chicago	Marquette University	Purdue University
University of Cincinnati	Michigan State University	Saint Louis University
Illinois Institute of Technology	The University of Michigan	Southern Illinois University
University of Illinois	University of Minnesota	The University of Texas at Austin
Indiana University	University of Missouri	Washington University
Iowa State University	Northwestern University	Wayne State University
The University of Iowa	University of Notre Dame	The University of Wisconsin

#### NOTICE

This report was prepared as an account of work sponsored by the United States Government. Neither the United States nor the United States Department of Energy, nor any of their employees, nor any of their contractors, subcontractors, or their employees, makes any warranty, express or implied, or assumes any legal liability or responsibility for the accuracy, completeness or usefulness of any information, apparatus, product or process disclosed, or represents that its use would not infringe privately-owned rights. Mention of commercial products, their manufacturers, or their suppliers in this publication does not imply or connote approval or disapproval of the product by Argonne National Laboratory or the U. S. Department of Energy.

ANL/NDM-44

THE INTERACTION OF FAST NEUTRONS WITH  $^{60}\text{Ni}^*$

by

A. Smith, P. Guenther,  
D. Smith and J. Whalen

January 1979

Applied Physics Division  
Argonne National Laboratory  
9700 South Cass Avenue  
Argonne, Illinois 60439  
USA

## NUCLEAR DATA AND MEASUREMENTS SERIES

The Nuclear Data and Measurements Series presents results of studies in the field of microscopic nuclear data. The primary objective is the dissemination of information in the comprehensive form required for nuclear technology applications. This Series is devoted to: a) measured microscopic nuclear parameters, b) experimental techniques and facilities employed in measurements, c) the analysis, correlation and interpretation of nuclear data, and d) the evaluation of nuclear data. Contributions to this Series are reviewed to assure technical competence and, unless otherwise stated, the contents can be formally referenced. This Series does not supplant formal journal publication but it does provide the more extensive information required for technological applications (e.g., tabulated numerical data) in a timely manner.

TABLE OF CONTENTS

	<u>Page</u>
ABSTRACT. . . . .	1
I. INTRODUCTION. . . . .	2
II. MEASUREMENT METHODS . . . . .	3
A. Measurement Sample. . . . .	3
B. Neutron Total Cross Sections. . . . .	3
C. Neutron Scattering Measurements . . . . .	5
D. (n;n', $\gamma$ ) Measurements . . . . .	6
III. EXPERIMENTAL RESULTS. . . . .	7
A. Neutron Total Cross Sections. . . . .	7
B. Neutron Elastic Scattering. . . . .	9
C. Neutron Inelastic Scattering. . . . .	13
IV. INTERPRETATION. . . . .	20
V. CONCLUDING REMARKS. . . . .	30
ACKNOWLEDGEMENTS. . . . .	31
REFERENCES. . . . .	32

THE INTERACTION OF FAST NEUTRONS WITH  $^{60}\text{Ni}$ \*

by

A. Smith, P. Guenther,  
D. Smith and J. WhalenArgonne National Laboratory  
Argonne, Illinois

## ABSTRACT

Neutron total cross sections of  $^{60}\text{Ni}$  are measured with broad resolutions from  $\sim 0.5$  to 5.0 MeV at intervals of  $\sim 50$  keV. Differential elastic-neutron-scattering cross sections are measured from 1.5 to 4.0 MeV at intervals of  $\sim 50$  keV over the scattered-neutron angular range of  $\sim 20$ -160 deg. Differential cross sections for the inelastic-neutron excitation states at  $1.342 \pm 0.013$ ,  $2.168 \pm 0.010$ ,  $2.304 \pm 0.026$ ,  $2.509 \pm 0.022$ ,  $2.636 \pm 0.019$  and  $3.164 \pm 0.041$  MeV are measured. The experimental results are interpreted in terms of optical-statistical and coupled-channels models including consideration of compound-nucleus fluctuations and direct-vibrational processes.

\*This work supported by the U.S. Department of Energy.

## I. INTRODUCTION

Nickel is a major constituent of radiation resistant stainless steel and 26% of the element consists of the isotope  $^{60}\text{Ni}$ . Thus fast-neutron cross sections of  $^{60}\text{Ni}$  are a concern in the neutronic design of many fast-reactor and fusion energy systems. The desired accuracies of the elemental fast-neutron scattering cross sections of nickel are  $\sim 5\%$ .<sup>1</sup> Measurements of fast-neutron scattering cross sections to such accuracies are most promising when undertaken isotope by isotope. The present measurements follow this approach in an effort to obtain fast-neutron total and scattering cross sections to accuracies of  $\sim 5\%$  and with energy resolutions sufficient to define intermediate resonance structure.

The neutron interaction with  $^{60}\text{Ni}$  in the few-MeV region is a mixture of compound-nucleus and direct-reaction processes. The compound-nucleus contribution is characterized by resonance effects not well resolved in measurements. Interpretation of the measured results in the context of energy-averaged models requires an extensive data base to reasonably assure a measurement of the actual energy-averaged behavior of the processes. Such a broad data base was sought in the present measurements. The experimental results were interpreted in terms of compound-nucleus and coupled-channels models with attention to resonance fluctuations and direct-vibrational processes. Both of these aspects of the neutron interaction in the present mass-energy region are shown to make significant contributions to the observed cross sections.

## II. MEASUREMENT METHODS

### A. Measurement Samples

The scattering and total cross section measurements employed a single cylindrical sample of metallic nickel 2 cm in diameter and 2 cm long enriched to  $\sim 99.6$  weight-percent in  $^{60}\text{Ni}$ .<sup>2</sup> The contributions of minor isotopic components of the sample to the present experimental results were estimated, found negligible and ignored. Chemical impurities in the sample were negligible and ignored. The sample was assumed to be of uniform density and this assumption was supported by qualitative tests (e.g. weight and balance). However, it was not possible to destroy the sample in order to verify its uniformity. The  $(n;n',\gamma)$  measurements employed an elemental nickel sample 3.8 cm long and 3.8 cm in diameter.

### B. Neutron Total Cross Sections

The neutron total cross section measurements were made using the monoenergetic-source facilities at the Argonne National Laboratory Fast Neutron Generator.<sup>3,4</sup> The neutron source was the  $^7\text{Li}(p;n)^7\text{Be}$  reaction produced by a proton burst of  $\sim 1$  nsec duration incident on a lithium metal film at a repetition rate of 2 MHz. The energy of the resulting neutrons was governed by the proton energy and the neutron-energy resolution was controlled by the thickness of the lithium-target film. A shield and associated collimator around the source were used to obtain a neutron beam  $\sim 1$  cm in diameter at a zero-degree source-reaction angle. The nickel sample was placed upon a wheel so that it rotated through the beam

at a repetition rate of approximately 20 rpm. Alternately, a void and a carbon-reference sample were placed in the beam. In all cases the neutron beam was incident on the bases of the cylindrical samples. The neutron detector was a proton-recoil scintillator placed on the neutron-beam axis approximately 5 m from the neutron source. Conventional time-of-flight techniques were used to obtain the velocity spectra of neutrons arriving at the detector. The observed spectra were correlated with the sample (or void) positions using an on-line computer system. The rapid interchange of sample positions avoided any necessity for monitoring the neutron-source intensity. The prominent neutron peak observed in the velocity spectra corresponding to the primary yield of the source reaction was integrated to obtain the detector response rate. The velocity resolution of the apparatus was sufficient to permit clear rejection of the secondary (and minor) neutron group from the source reaction. Backgrounds were small and easily determined from an analysis of the velocity spectra. A random signal was introduced into the data acquisition system in order to determine dead-time corrections precisely. In-scattering corrections were estimated and found to be negligible. The neutron transmissions through the samples followed directly from the observed detector responses. The total cross sections were calculated from the transmissions in the conventional manner.<sup>5</sup> An ancillary experiment utilized the same apparatus to determine the neutron total cross sections of sulfur, silicon and carbon over selected energy intervals with resolutions of 2-5 keV. The results were correlated with well known resonance structure in these elements in order to determine the energy scale of the apparatus to within  $\sim 10$  keV; i.e. to values approximately an order of magnitude less than the resolutions employed in the present nickel measurements.<sup>6,7,8</sup>

Details of the above method and the particular apparatus are given in Ref. 4.

### C. Neutron Scattering Measurements

The neutron scattering measurements were made using the Argonne National Laboratory 10-angle, pulsed-beam time-of-flight system.<sup>9</sup> The  ${}^7\text{Li}(p;n){}^7\text{Be}$  neutron source was pulsed on for durations of  $\sim 1$  nsec at a repetition rate of 2 MHz. The mean incident-neutron energy at the scattering sample was known to  $\sim 10$  keV by control of the proton beam. The scattering sample was placed  $\sim 13$  cm from the neutron source at a zero-degree reaction angle. Proton-recoil scintillators were placed at flight paths of 5 to 5.5 m, measured from the scattering sample. The flight paths were defined by a massive collimator system extending over a scattered-neutron angular range of 20 to 160 deg. The scattering angles were determined to a relative accuracy of  $\sim 0.5$  deg. and an absolute accuracy of  $\sim 1.0$  deg. An independent time-of-flight system was used to monitor the source intensity, supported by four "long counters." The relative energy dependencies of the scattered-neutron-detector sensitivities were determined by observation of neutrons scattered from hydrogen (polyethylene) at selected angles and a fixed incident energy or from measurements of the neutron spectrum emitted during the spontaneous fission of  ${}^{252}\text{Cf}$ .<sup>10</sup> The normalizations of the relative-detector sensitivities were determined by observing neutrons scattered from hydrogen (polyethylene) at selected energies and angles. Thus all scattering cross sections were determined relative to well known  $\text{H}(n;n)$  cross sections.<sup>11</sup> Data acquisition was carried out using on-line computer systems with data storage in a 512 (time intervals) by 16 (detector energy-response intervals) by 11 (10 scattering and 1 monitor detectors) matrix. Subsequent data processing

reduced the measured velocity spectra to differential cross sections and included corrections for angular resolution, sample attenuation and multiple-event effects.<sup>12</sup> The corrections employed both analytical and Monte-Carlo procedures and were applied to  $^{60}\text{Ni}$ , polyethylene (hydrogen) and carbon-reference samples. The latter were used to verify the fidelity of the measurement system by comparing measured carbon cross sections with standard values reported in the literature.<sup>13</sup> Details of the above method and the specific apparatus have been extensively described elsewhere.<sup>9,12</sup>

#### D. (n;n', $\gamma$ ) Measurements

In addition to the above direct neutron detection method, the (n;n', $\gamma$ ) reaction was examined at energies of  $\sim 2.0$  MeV using an elemental sample in order to extend the prominent neutron first-inelastic excitation to threshold. The gamma rays were detected using GeLi detectors and the relative neutron flux determined using a  $^{235}\text{U}$  fission chamber as described in Refs. 14 and 19. Measurements were made at a gamma-ray emission angle of 55 deg. with incident neutron energy resolutions of  $\sim 75$  keV. The shape of the angle integrated (n;n', $\gamma$ ) cross section was deduced by multiplying the measured 55 deg. values by  $4\pi$ . This procedure is not precisely valid, since  $P_4$  contributions to the angular distributions are allowed and may not be negligible particularly near threshold (e.g. see Ref. 19). However, the  $P_4$  contribution is probably <10% over most of the range of the present data thus the contribution was neglected in the absence of detailed angular-distribution information. The measured relative gamma-ray excitation function was subsequently normalized to the directly measured neutron-scattering results in the region of overlap near 2.0 MeV. Throughout the energy range of the (n;n', $\gamma$ ) measurements only one inelastic-scattering channel was open; thus there were no uncertainties due to the interpretation of gamma-ray branching ratios.

### III. EXPERIMENTAL RESULTS

#### A. Neutron Total Cross Sections

The objective of the total cross-section measurements was the determination of precise energy-averaged magnitudes comparable with the subsequently measured scattering cross sections and model predictions. Resolution of the detailed resonance structure was explicitly avoided. The measurements were made from 0.5 to 5.0 MeV at intervals of  $\sim 50$  keV with resolution of  $\geq 50$  keV. The measurements were repeated over the entire energy range several times with consistent results. Moreover, the concurrent measurement of the neutron total cross sections of carbon provided results in good agreement with those reported in the literature.<sup>6</sup> The experimental values were averaged over intervals of 200 keV to obtain the energy-averaged results shown in Fig. 1. The statistical accuracies of the 200 keV-average cross sections were generally  $\sim 1\%$ . Even with the relatively large averaging increment cross-section fluctuations remained evident and complicated comparisons with the measured scattering cross sections and the physical interpretations.

The present results are compared with equivalent average values constructed from the much better resolution results of Clement et al.<sup>15</sup> in Fig. 1. The two sets of results are generally consistent to within several percent at incident energies  $> 1.5$  MeV. At lower energies, resonance perturbations in broad resolution measurements using the present sample (2 cm thick) can be significant. Their effect was estimated using Monte-Carlo and analytical methods, assuming that essentially all the resonances were perfectly resolved in the measurements of Ref. 15. With this assumption the estimated perturbation was negligibly small at  $\sim 2.0$  MeV and increased

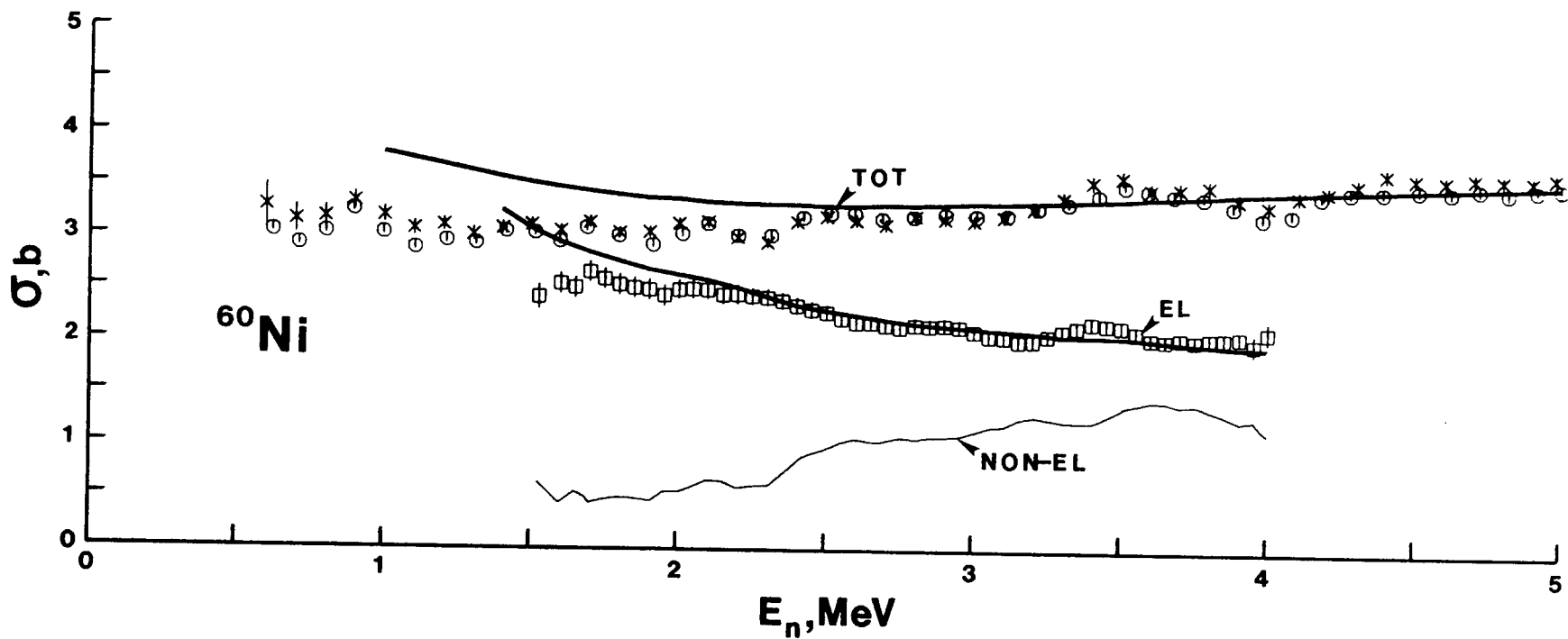


Fig. 1. Neutron Total and Elastic-Scattering Cross Sections of  $^{60}\text{Ni}$ . 200 keV averages of the present results are indicated by  $\circ$  and  $\square$  symbols, respectively. Comparable averages of the neutron total cross sections of Ref. 15 are noted by crosses. Curves indicate the results of model calculations and the non-elastic scattering cross section deduced from the present measurements.

to  $\sim 5\%$  as the energy decreased to 0.5 MeV. This estimate is qualitatively consistent with the low-energy differences between the present results and those derived from Ref. 15 as evident in Fig. 1. These estimates are certainly lower limits as the resolution used in Ref. 15 was not perfect. Theoretical estimates suggest that the resonance structure at  $\sim 2.0$  MeV, including the cross section minima, is far more pronounced than observed in any reported measurements.<sup>16</sup> As an illustration, the structure observed in Ref. 15 was "enhanced" by squaring the measured values and renormalizing to the original average magnitudes. The estimated perturbations deduced from these "enhanced" cross sections were  $\sim 20\%$  at 0.5 MeV and smoothly decreased to small values at 2.0 MeV. The same perturbations could be experimentally determined using various sample thicknesses. However, such procedures would have compromised a unique sample and thus were not attempted.

The above considerations suggest that the present energy-averaged neutron total cross sections are quantitatively representative of the microscopic values at energies of  $\sim 1.5$  MeV. Below  $\sim 1.5$  MeV the measured energy-averaged transmissions may lead to total cross sections as much as  $\sim 20\%$  too small depending on the incident energy and the unknown details of the true resonance structure, particularly near the resonance minima. The effect of sample size in the measurement of energy-averaged neutron total cross sections has been discussed in greater detail elsewhere.<sup>4</sup> The importance of sample-size perturbations in the measurement of highly resonant cross sections is too seldom recognized.

#### B. Neutron Elastic Scattering

Elastic neutron scattering cross sections were measured at incident energy intervals of  $\leq 50$  keV from 1.5 to 4.0 MeV with incident-energy

resolutions of  $\sim 20$ -40 keV. Measurements were made at ten or more scattering angles, distributed between 20 to 160 deg. for each incident energy. The objective was an angle-energy scope that would well define the elastic scattering cross sections to an intermediate energy resolution. The measurements were made at randomly selected energies or systematically over a pre-determined energy range during various measurement periods. Carbon-scattering measurements were made concurrently to assure the fidelity of the apparatus. The individual differential scattering cross sections were generally determined to 5 to 8% accuracies. Statistical uncertainties contributed 1-3% to the overall uncertainties. Correction procedures, including those for effects due to angular uncertainties, made a similar small contribution. The largest contribution to the overall uncertainty came from the calibration of the detector efficiency (typically 3 to 5%). The uncertainty in the H(n;n) standard was a small factor (e.g.  $\lesssim 1\%$ ).

The experimental results are outlined in Fig. 2. Despite the relatively-broad incident-energy resolutions, considerable variation in the distributions with energy is discernable throughout the measured energy range. Any single distribution is not necessarily representative of the more general energy-averaged behavior. A better representation of the average behavior is obtained by averaging the measured values over 200-keV intervals with results as illustrated in Fig. 3. With this 200-keV average, the behavior of the distributions vary relatively smoothly with energy, and is comparable with predictions of the energy-averaged models.

The 200-keV averages of the present results were least-square fitted with a Legendre polynomial expansion from which the angle-integrated elastic-scattering cross sections were derived. The accuracies of the latter were

Fig. 2. Illustrative Differential Elastic-Neutron Scattering Cross Sections of  $^{60}\text{Ni}$ . Incident-energy resolutions are 20-40 keV. Curves are the results of least-square fitting of Legendre-polynomial expansions to the actual measured values. Fluctuations with energy are evident. (Scattering angle in laboratory degrees, cross-sections in b/sr.)

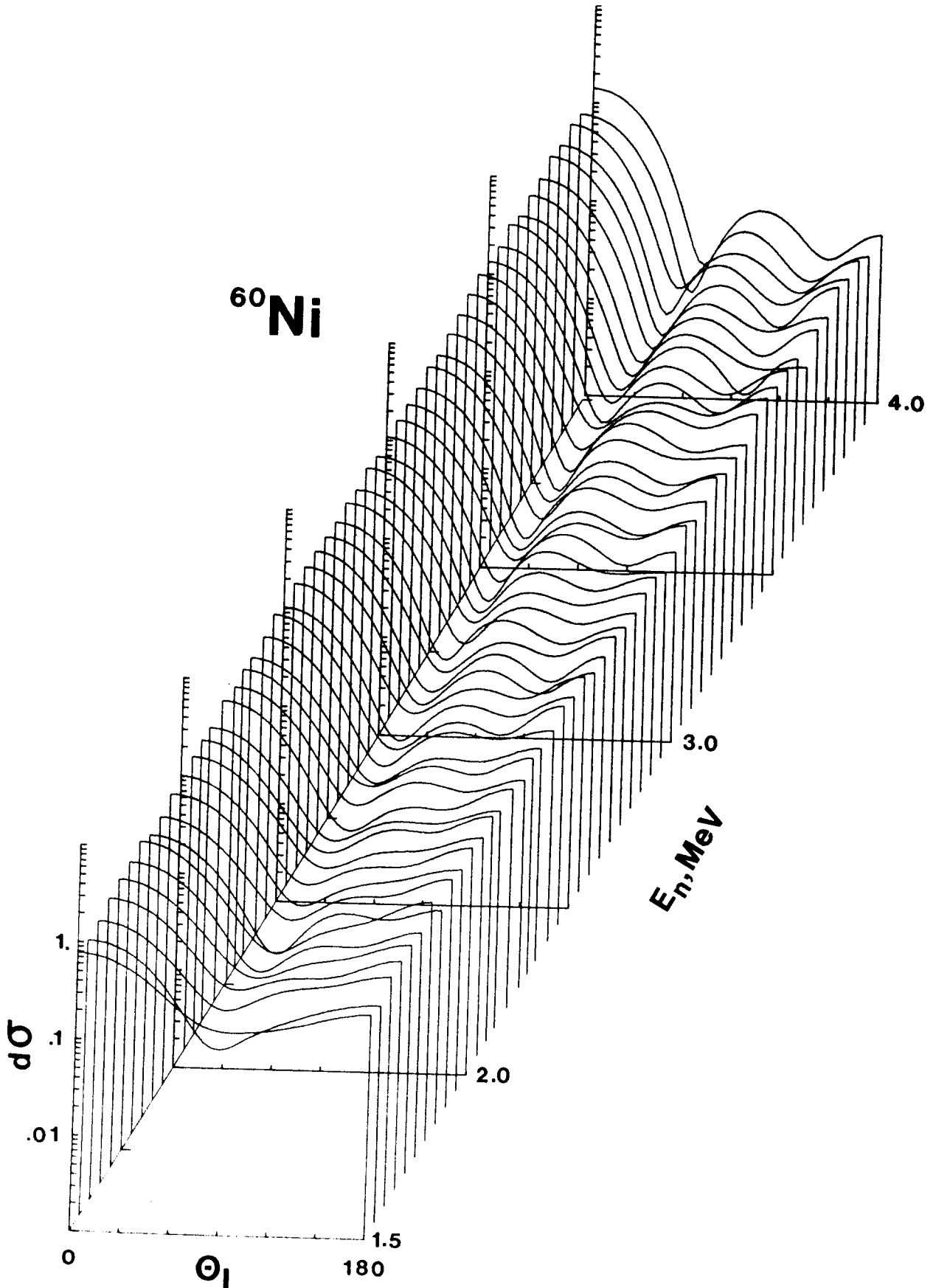
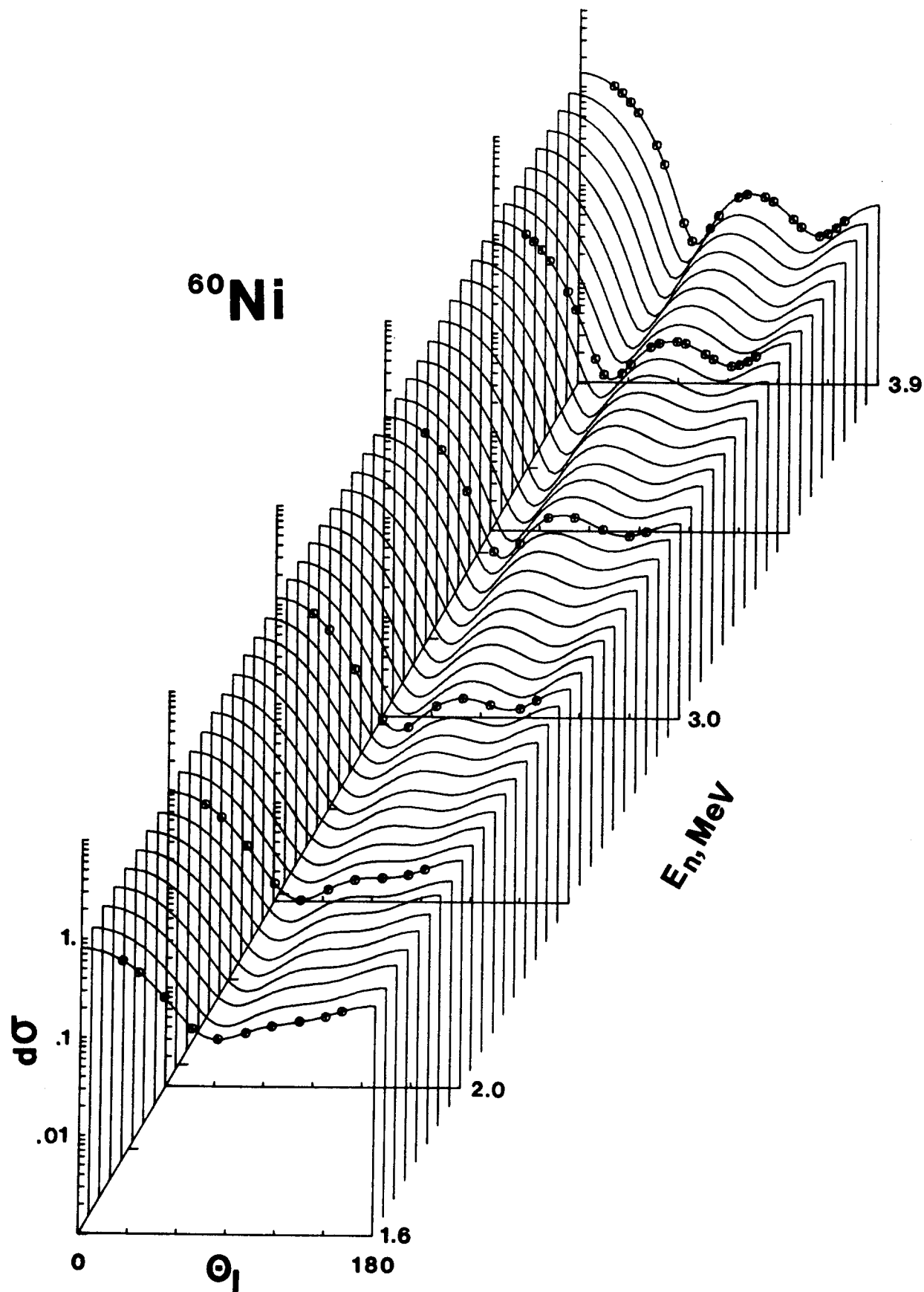


Fig. 3. 200-keV Average of the Measured Neutron Differential Elastic-Scattering Cross Sections of  $^{60}\text{Ni}$ . Curves indicate the results of a least-square fitting of Legendre-polynomial expansions to the measured values. Illustrative data points are shown. (Scattering angle in laboratory degrees, cross section in mb/sr.)



generally  $\leq 5\%$ , i.e. essentially dominated by the uncertainties associated with detector calibrations. These elastic-scattering cross sections are compared with the neutron total cross in Fig. 1. The angle-integrated elastic scattering cross sections fluctuate with energy in a manner consistent with the fluctuations of the neutron total cross sections. Together the two sets of cross sections yield the non-elastic cross sections shown in Fig. 1. Above  $\sim 2.0$  MeV the non-elastic cross sections were consistent with the directly-measured neutron inelastic scattering cross sections while at lower energies they tended to be somewhat smaller, consistent with the total neutron cross section perturbations discussed above.

There appear to be no previously reported elastic scattering results with which to compare the present measured values.

### C. Neutron Inelastic Scattering

Differential-neutron-inelastic-scattering cross sections were determined concurrently with the elastic-scattering values. Scattered neutrons were observed corresponding to levels in  $^{60}\text{Ni}$  at:  $1.343 \pm 0.013$ ,  $2.168 \pm 0.010$ ,  $2.304 \pm 0.026$ ,  $2.509 \pm 0.022$ ,  $2.636 \pm 0.019$  and  $3.164 \pm 0.041$  MeV. The excitation energies were determined from the measured incident energies, flight times and flight paths and were verified by the observation of well known inelastic-neutron groups (e.g. that due to excitation of the 846 keV level in  $^{56}\text{Fe}$ ). The above measured excitation energies are averages of a number of independent measurements and the uncertainties are RMS deviations from the mean. The presently-observed levels correspond reasonably well to known states in  $^{60}\text{Ni}$  as shown by the comparisons of Table 1.<sup>17</sup> The correspondence is explicit to an excitation energy of  $\sim 3.0$  MeV. The observed 3.164 MeV level is attributed to a composite of three closely-spaced reported states.

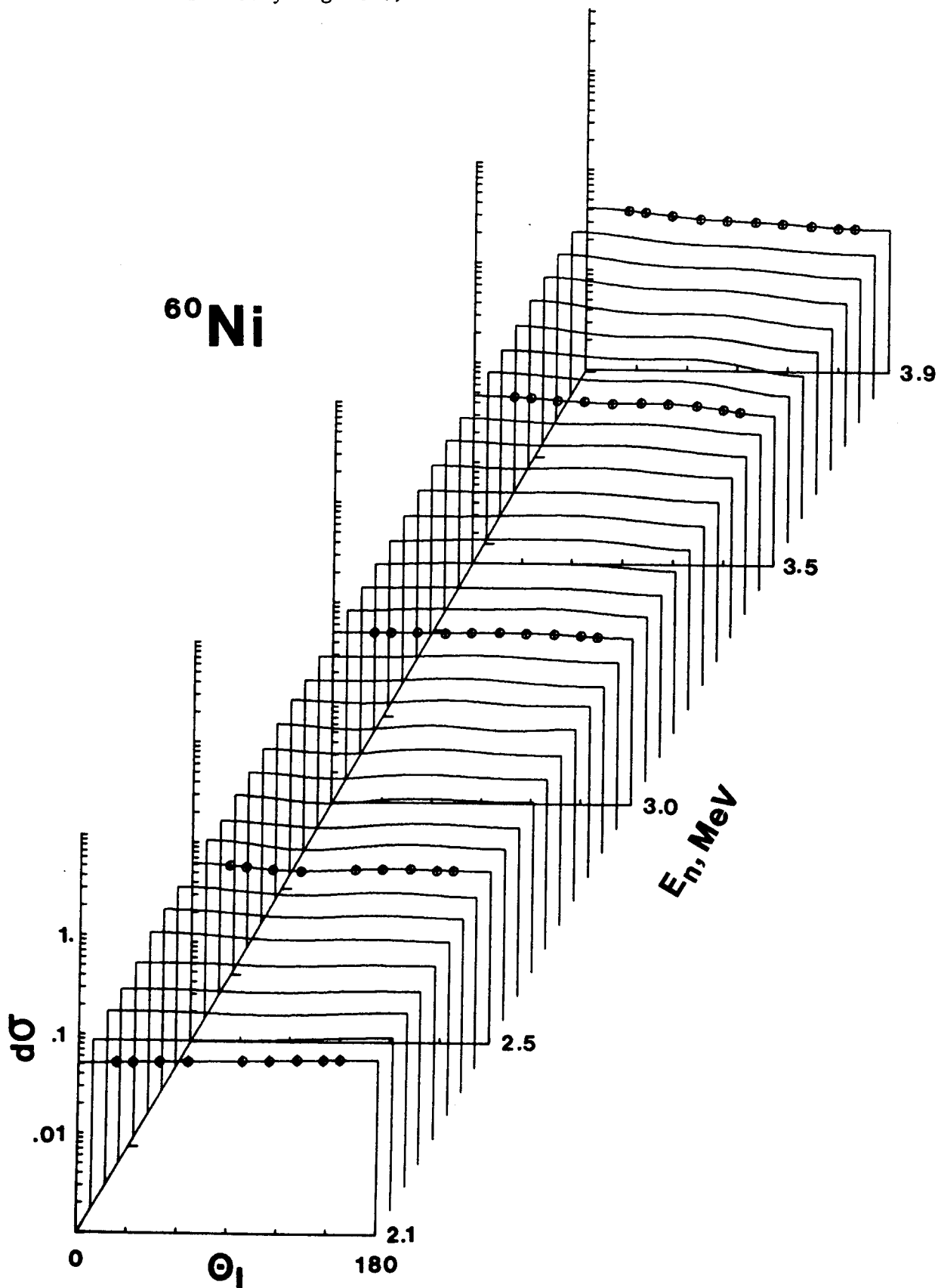
TABLE 1. Comparison of Observed and  
Reported Levels in  $^{60}\text{Ni}$

<u>No.</u>	<u><math>E_x</math> (MeV), Observed</u>	<u><math>E_x</math> (MeV), Ref. 17</u>
1	$1.342 \pm 0.013$	1.333 (2+)
2	$2.168 \pm 0.010$	2.158 (2+)
3	$2.304 \pm 0.026$	2.296 (0+)
4	$2.509 \pm 0.022$	2.506 (4+)
5	$2.636 \pm 0.019$	2.625 (3+)
6	$3.164 \pm 0.041$	<div style="border: 1px solid black; padding: 2px; display: inline-block;">           3.123 (2+)            3.184 (?)            3.195 (1+)         </div>

Angle-integrated neutron inelastic-excitation cross sections were determined by least-square fitting no fewer than four differential values at each energy with Legendre polynomial series. The uncertainties in the differential-cross section values ranged from a minimum of  $\sim 5\%$  for prominent and well-resolved neutron groups at favorable energies to  $\sim 20\%$  for less well resolved and/or low-intensity neutron groups. There was a similar spread in the uncertainties of angle-integrated cross sections ranging upward from a minimum of  $\sim 5\%$ . In addition to the complexities of experimental resolution and lesser experimental intensities, the inelastic-scattering uncertainties were subject to the same sources of uncertainty noted above in the elastic-scattering context.

A major feature of the inelastic process is the prominent excitation of the 1.342 MeV one-phonon vibrational state. The differential cross sections for the excitation of this state fluctuate with energy in a manner analogous to that illustrated for the elastic scattering cross sections in Fig. 2. Fluctuations were also observed in the excitation of higher levels. However, the incident energies were larger so the effect was not as pronounced as in the case of the 1.342 MeV level. In order to remove these fluctuations the measured inelastic scattering distributions were averaged over 200 keV incident-neutron energy intervals in the same manner as for to the elastic-scattering distributions (see above discussion). The resulting averages behaved in a relatively smooth manner as illustrated by the distributions for the 1.342 MeV state shown in Fig. 4. Furthermore, this figure qualitatively shows the trend from distributions symmetric about 90 deg. at lower energies to those that are somewhat peaked forward at upper energies in a manner that could be expected as the result of increasing contributions from direct-reaction processes. Cross sections for the excitation of

Fig. 4. Observed Differential Cross Sections for the Inelastic Excitation of the 1.342 MeV Level in  $^{60}\text{Ni}$ . Measured values are illustrated by data points and curves denote a  $P_4$  Legendre polynomial fit to the measured values. (Cross sections are in b/sr and scattering angle in laboratory degrees.)



higher-lying levels also fluctuated, and averaging procedures were used to obtain the energy-averaged behavior in the same fashion as outlined above for the 1.342 MeV level. Scattered neutron distributions resulting from the excitation of these higher-lying levels were generally symmetric about 90 deg. (see Fig. 7 for illustrative examples).

The above direct-neutron measurements extended to within  $\sim 0.8$  MeV of threshold.  $(n;n',\gamma)$  techniques were used to extend the measured cross sections for the excitation of the prominent 1.342 MeV to threshold. The measured relative  $(n;n',\gamma)$  results were normalized to the directly measured  $(n;n')$  values near 2.0 MeV. The normalization region is one of fluctuating cross sections so it is estimated that the  $(n;n',\gamma)$  normalization uncertainty is  $\sim 10\%$ .

The angle-integrated neutron inelastic scattering cross sections derived from the direct neutron measurements are shown in Fig. 5 together with the values obtained from the  $(n;n',\gamma)$  measurements. There is very little previously-reported comparable information explicitly deduced from measurements using isotopic  $^{60}\text{Ni}$  samples. There are a number of results of both  $(n;n')$  and  $(n;n',\gamma)$  measurements employing elemental nickel targets. Some of these latter results are shown in Fig. 5. The recent high-resolution gamma-ray-emission results of Voss<sup>18</sup> show the same qualitative fluctuations as the present work when averaged over 75-100 keV. There is a difference in cross section magnitudes for the excitation of the 1.342 MeV level at energies of  $\sim 2.1$  MeV, where the interpretation of the gamma-ray cross sections is unambiguous, possibly reflecting the angular distribution of the gamma-ray emission in the context of the 125 deg. measurement angle of Ref. 18. The present results are in reasonably good agreement with those obtained from the elemental studies of Ref. 20. There

Fig. 5. Inelastic Neutron Excitation Cross Sections of  $^{60}\text{Ni}$ . The present (n;n') results are noted by solid circular symbols, those from (n;n', $\gamma$ ) measurements by solid square symbols. Other symbols denote previously reported values as given in Refs. 20-26. Light curves indicate a 75 keV average of the gamma-ray emission cross sections of Ref. 18 with the energy of the gamma-ray observed noted with the respective curve. Level excitation energies are numerically stated at the left of each section of the figure. Dashed curves indicate corresponding ENDF/B-IV values.<sup>28</sup> Heavy solid curves denote results of model calculations as outlined in Sec. IV of the text ("D" = result of deformed model, "S" or no notation = spherical model). (Figure on following page.)

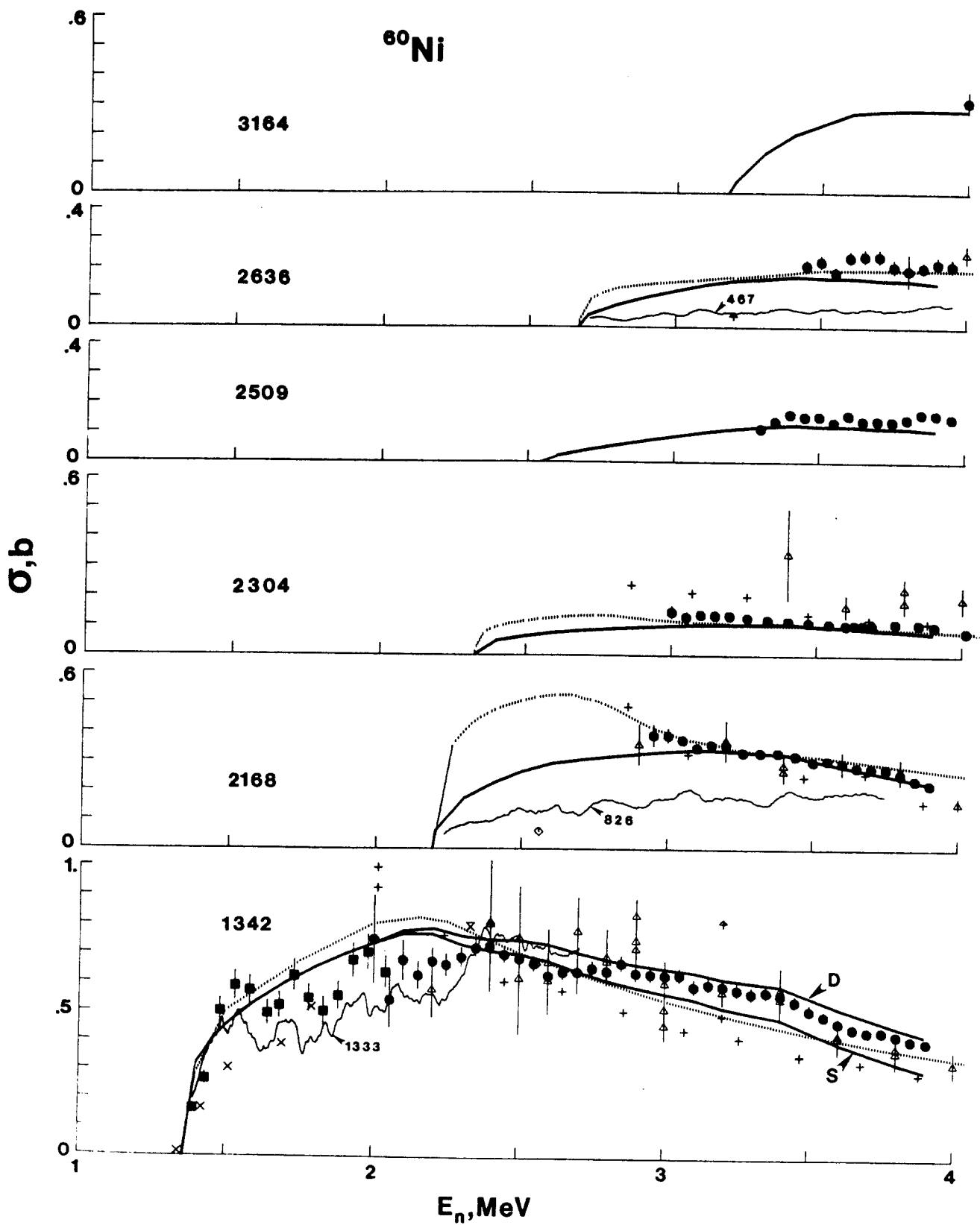


Fig. 5

seem to be systematic differences between the results of the present work and those of Ref. 21. Other scattered results from Refs. 22 to 26 vary from rather good agreement to sharp disagreement with the present values. The present results are very consistent with an extrapolation of the higher-energy results of Kinney and Perey<sup>27</sup> obtained with isotopically enriched samples. The validity of comparisons of isolated values is questionable in view of the fluctuations in the cross sections and unavoidable variations in experimental energy scales and resolutions. In addition, there are ambiguities in the interpretation of the  $(n;n',\gamma)$  results (such as those of Ref. 24) beyond the excitation of the first several levels.

Some of the present neutron-inelastic-scattering results can be compared with values given in the elemental ENDF/B-IV nickel file, corrected to isotopic quantities. The comparisons, indicated in Fig. 5, suggest that those portions of the differential inelastic scattering file due to  $^{60}\text{Ni}$  are too large by 15-20% to  $\sim 3.0$  MeV. This difference exceeds the accuracies frequently requested for elemental nickel neutron inelastic-scattering cross sections.

#### IV. INTERPRETATION

The experimental interpretations sought to: a) establish a spherical optical potential providing an acceptable description of the energy-averaged neutron cross sections in this mass-energy region of strong fluctuations, and 2) explore the effect of direct-vibrational processes on the neutron interaction. The scope and detail of the present experiments provides a suitable foundation for such investigations.

The spherical optical potential was entirely based upon the 200 keV average of the measured differential elastic-scattering cross sections (i.e. the distributions shown in Fig. 3). The averaging increment was a compromise between a representation consistent with the concept of the optical model and the excited-level spacing influencing the compound-elastic component. The initial step in the deduction of the potential was a 6-parameter (real and imaginary strengths, radii and diffusenesses) Chi-square fit of a conventional surface absorption optical potential to each of the measured elastic-scattering distributions.<sup>29</sup> The compound-elastic contributions were calculated using the Hauser-Feshbach formula with width-fluctuation corrections<sup>30,31</sup> assuming the first 12 excited levels as defined in Ref. 17. The initial fitting procedures reasonably defined real and imaginary radii and diffusenesses. These four-parameters were then fixed for subsequent and more detailed two-parameter (real and imaginary strengths) Chi-square fitting procedures. The latter included the enhancement of compound-nucleus components using the formalism of Hofmann et al.,<sup>32</sup> explicit consideration of the levels defined in Table 1, and the level-density-distributions of Gilbert and Cameron<sup>33</sup> for the description of levels with excitations of >3.2 MeV. The calculations were carried out using the computer code ABAREX-2.<sup>34</sup> The resulting V (real strength) and W (imaginary strength) followed a general linear energy dependence. V decreased at the rate of  $\sim 0.3$  MeV/MeV, consistent with previously reported values<sup>35</sup> and W increased at the rate of  $\sim 0.25$  MeV/MeV. Superimposed on these linear trends were relatively small ( $\sim \pm 1$  MeV) fluctuations with a periodicity of  $\sim 0.5$  MeV. These fluctuations reflected those of the underlying data base (as illustrated in Figs. 1 and 3).

The fluctuations were not characteristic of a general energy-averaged behavior and were ignored in the resulting "general potential" given in Table 2. This "general potential" was the basis for subsequent comparisons of measured and calculated values and the investigation of direct-vibrational processes.

The "general potential" provides an acceptable description of measured neutron-elastic-scattering cross sections as generally outlined in Fig. 6 and more specifically illustrated by the examples of Fig. 7. Differences between measured and calculated results are generally small and random in nature as might be expected from the residual fluctuations. In addition, there are systematic differences at energies  $\gtrsim 3.3$  MeV primarily associated with the first minimum of the diffraction pattern.

Above  $\sim 2.0$  MeV, measured and calculated angle-integrated elastic-scattering cross sections are consistent to within several percent, again with minor deviations due to fluctuations (see Fig. 1). Below  $\sim 2.0$  MeV the calculated values become somewhat larger with decreasing energy. In addition to fluctuations, doorway levels have been reported in this lower-energy region.<sup>36</sup> In view of these considerations the agreement of measured and calculated angle-integrated elastic scattering cross sections was judged acceptable.

Comparisons of measured and calculated neutron total cross sections follow the same trends as the angle-integrated elastic-scattering cross sections. Again, above  $\sim 2.0$  MeV the agreement is good, while at lower energies the calculated values become progressively larger amounting to differences of 10-15% at  $\sim 1.0$  MeV. In addition to the effects of fluctuations

TABLE 2. Spherical Optical-Potential Parameters

---

Real Potential<sup>a</sup>

Strength  $V = 53.10 - 0.3 \cdot E(\text{MeV}), \text{ MeV}$

Radius  $r_v = 1.211, \text{ F}$

Diffuseness  $a_v = 0.614, \text{ F}$

Imaginary Potential<sup>b</sup>

Strength  $W = 7.90 + 0.25 \cdot E(\text{MeV}), \text{ MeV}$

Radius  $r_w = 1.202, \text{ F}$

Diffuseness  $a_w = 0.596, \text{ F}$

---

<sup>a</sup>Saxon form.

<sup>b</sup>Saxon derivative form.

\*Spin-orbit terms of Thomas form and 8 MeV strength included in all calculations.

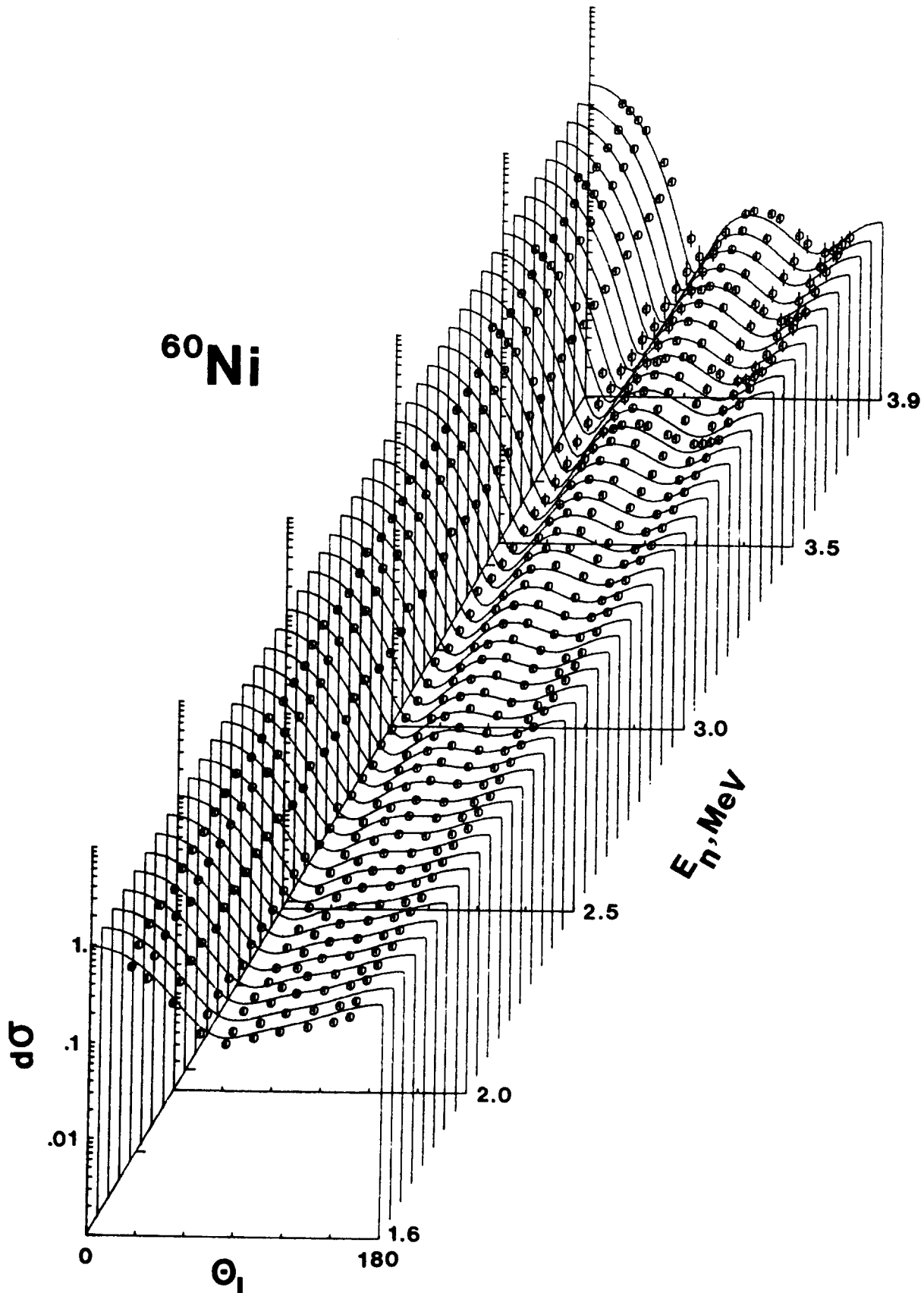


Fig. 6. Comparison of Measured (Data Points) and Calculated (Curves) Differential Elastic-Scattering Cross Sections of  $^{60}\text{Ni}$ . (Cross sections are given as b/sr and angles as degrees in the lab system.)

Fig. 7. Illustrative Comparisons of Measured and Calculated Differential Scattering Cross Sections of  $^{60}\text{Ni}$ . Measured values are indicated by data points where:  $\square$  = elastic scattering,  $\circ$  =  $E_x$  of 1.342 MeV,  $\triangleleft$  =  $E_x$  of 2.168 MeV,  $+$  =  $E_x$  of 2.304 MeV,  $x$  =  $E_x$  of 2.509 MeV and  $\diamond$  =  $E_x$  of 2.636 MeV. Curves indicate the results of calculations where coupled-channels results are noted with "tick" marks and spherical results with simple curves. Incident energies are given in each section of the figure in MeV. Dimensionality is cross sections in b/sr and scattering angle in lab. degrees. (Figure on following page.)

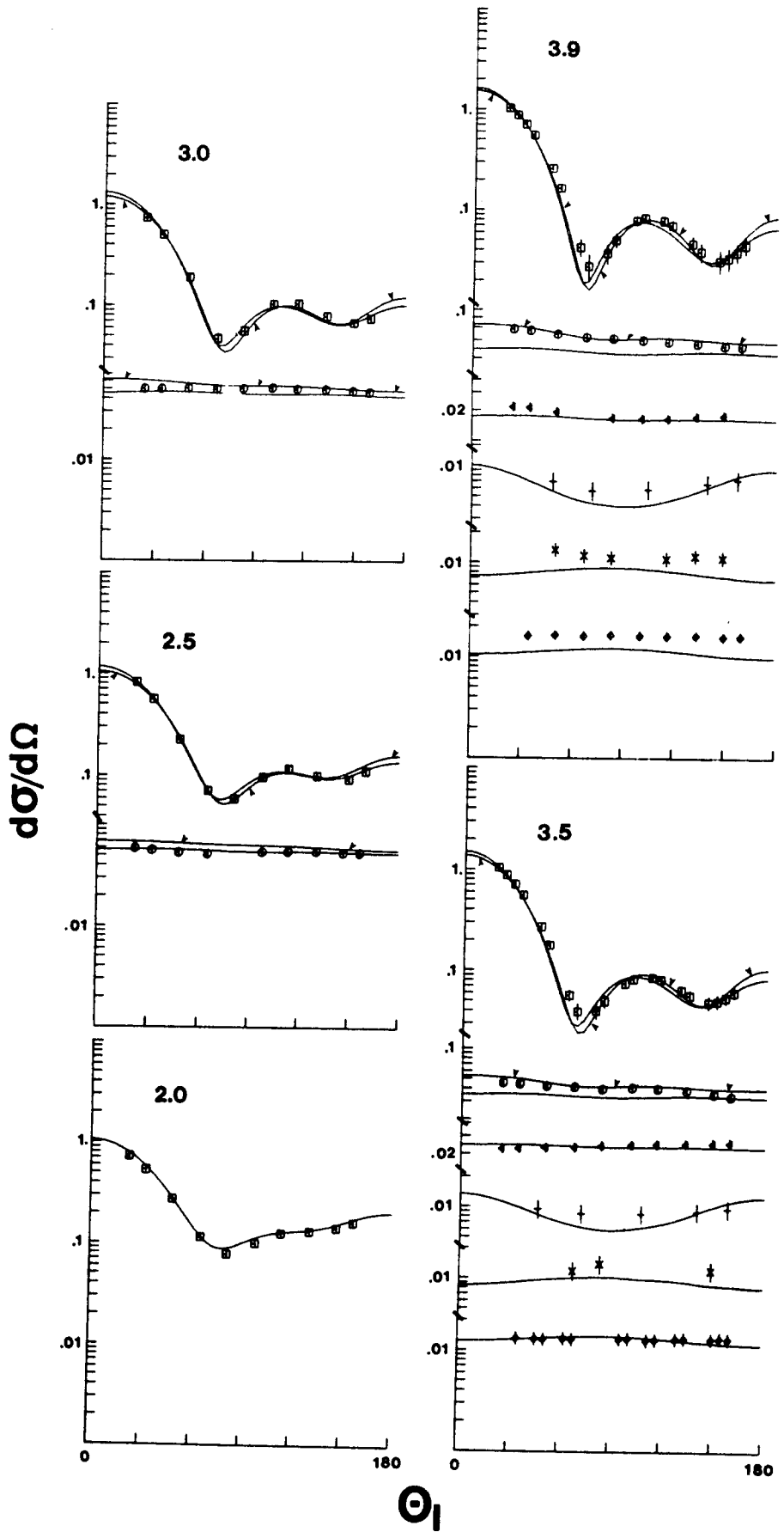


Fig. 7

and doorway levels there is the problem of experimental sample-size perturbations discussed in Sec. III, above. The differences between measured and calculated values are within the range of estimated experimental perturbations, alone. The inability of optical potentials based upon higher-energy elastic scattering to describe neutron total cross sections near 1.0 MeV in this mass region has long been observed. As outlined in Sec. III, much of this discrepancy may be experimental in origin, but there may also be a shortcoming in the concept of a simple spherical optical potential. In either event, there remains an uncertainty in energy-averaged neutron total cross sections in this mass-energy region of  $\sim 10\%$  in a number of nuclides. This can be a serious concern in the contexts of energy-average models and of the provision of evaluated data sets for technological purposes.

The neutron-inelastic-scattering cross sections calculated using the spherical "general potential" were qualitatively descriptive of the measured values (as illustrated in Figs. 5 and 7) but there were quantitative discrepancies. The calculated excitation of the 1.342 MeV (2+) level tends to be larger than the measured values below  $\sim 2.5$  MeV and smaller above  $\sim 3.0$  MeV. These differences are  $\sim 10-30\%$ . In addition, the calculated angular distributions of scattered neutrons do not show the forward peaking observed at higher energies. Calculated and measured cross sections for the excitation of the 2.168 MeV (2+) level are in very good agreement. Calculated excitations of the 2.304 MeV (0+) level are reasonably consistent with measured values but the calculated angular distributions are more anisotropic than observed experimentally. The measured differential cross sections are small ( $< 10$  mb/sr) and, as a consequence, relatively uncertain. Thus the measured values may not fully portray the concave angular distributions characteristic of this

0+ to 0+ transition. The measured cross sections for the excitation of the 2.509 MeV (4+) level agree to within 10-15% with the calculated values. However, the measured values for the excitation of the 2.636 MeV (3+) level are about 25% larger than the calculated quantities. This relatively large difference suggests an error in the assigned J- $\pi$  values. Indeed, a 2+ assignment results in better agreement with measured values but is inconsistent with the results of reported stripping-reaction studies.<sup>17</sup> The cross sections for the excitation of the observed level at 3.164 MeV were attributed to contributions from reported 3.123, 3.184 and 3.195 MeV levels. With this assumption the calculated cross sections were very similar to the limited number of measured values obtained in the present experiments.

At higher incident energies (e.g.  $\gtrsim 3.0$  MeV) the above spherical interpretations has three shortcomings; a) the calculated excitation of the 1.342 MeV level is systematically smaller than the measured values, b) measured neutron distributions resulting from the excitation of the 1.342 MeV level are not symmetric about 90 deg. as predicted by theory, and c) the measured elastic-neutron distributions deviate systematically from the calculated values as 4.0 MeV is approached. It is difficult to attribute these shortcomings entirely to fluctuations and/or the level-density approximation employed in the calculations. However, qualitatively the above characteristics are characteristic of direct-vibrational processes. Coulomb-excitation and stripping studies indicate that the first excited (1.342 MeV) level is a one-phonon vibrational state characterized by a  $\beta_2$  value of  $\sim 0.22$ .<sup>17,37</sup> The effect of the vibrational interaction was estimated using a coupled-channels calculation, coupling the ground (0+) and first-excited states assuming the above  $\beta_2$  value. The calculations were carried

out using the coupled-channel computer program JUPREX.<sup>38</sup> In doing so it was assumed that direct and compound-nucleus processes were approximately separable and that the latter could be reasonably calculated using transmission coefficients derived from the spherical potential. The "general potential" of Table 2 was used for the vibrational calculations except for the imaginary strength which was adjusted to improve the description of the observed differential elastic-scattering distributions. The vibrational calculations were an approximation in that they did not derive transmission coefficients directly from the deformed potential nor was there an attempt made to explicitly Chi-square fit the measured elastic distributions using the deformed potential. Such procedures would have been very costly and deceptive if applied to only a few measured distributions.

The coupled-channels results mitigated the shortcomings of the spherical results. The calculated distributions of neutrons resulting from the excitation of the 1.342 MeV level were peaked forward in the manner of the measured values (see Fig. 7). The cross section magnitudes and the neutron differential-elastic-scattering distributions were in much better agreement with the measured values than those obtained from the spherical calculations (see Figs. 5 and 7). Thus the comparisons of measured and calculated values strongly suggest that direct-vibrational processes are significant in the neutron interaction with  $^{60}\text{Ni}$  in the present energy range. In particular they account for facets of the interaction not consistent with the spherical optical-statistical model. Consideration of direct-vibrational interactions does result in modifications of potential parameters relative to the spherical model (e.g.  $\sim 30\%$  reduction in imaginary strength) thus one can question the quantitative validity of parameter sets derived from spherical interpretations in this mass-energy range.

## V. CONCLUDING REMARKS

The present measurements provide a detailed knowledge of neutron total and scattering cross sections of  $^{60}\text{Ni}$  from  $\sim 1.5$  to 4.0 MeV. A prominent feature of the experimental results is the strong fluctuations. These imply a need for a comprehensive data base for the precise determination of energy-averaged cross-section behavior. The present measurements do provide such a data base for interpretation in terms of energy-averaged models and for nuclear data for technological purposes. A conventional spherical optical potential, deduced from the measured values, quantitatively described the average experimental neutron total and scattering cross sections to energies of  $\sim 3.0$  MeV. A coupled-channels model considering direct-vibrational processes, extended the quantitative description of the measured results to 4.0 MeV. The direct-vibrational interaction significantly effected the choice of optical-model parameters. In this mass-energy range attention must be given to the scope of the data base if the experimental energy-averaged behavior, consistent with the concept of optical and coupled-channels models, is to be determined. The direct-vibrational process makes a significant contribution to the energy-averaged interpretation. These two considerations are often ignored in physical studies.

**ACKNOWLEDGEMENT**

The authors are indebted to Dr. P. A. Moldauer for his advice during this work and for providing computer programs used in this work.

## REFERENCES

1. WRENDA 74, World Request List for Nuclear Data Measurements, International Data Committee Report, INDC(SEC)-38/U (1974).
2. The authors are indebted to Mr. E. Kobisk for the fabrication of the essential research sample.
3. S. A. Cox and P. R. Hanley, IEEE Trans. Nucl. Sci., NS-18 No. 3, 108 (1971).
4. A. Smith and J. Whalen, Comments on Energy-Averaged Neutron Total Cross Sections, Argonne National Laboratory Report, ANL/NDM-33 (1977).
5. D. Miller, Fast Neutron Physics, Vol. II, Eds. J. Marion and J. Fowler, Interscience Pub., N.Y. (1963).
6. R. B. Schwartz, R. A. Schrack and H. T. Heaton, II, "MeV Total Neutron Cross Sections, U.S. Natl. Bur. Stds. Pub. NBS-138 (1974).
7. S. Cierjacks, P. Forti, D. Kopsch, L. Kropp, J. Nebe and H. Unfeld, "High Resolution Total Neutron Cross Sections between 0.5-30 MeV," Karlsruhe Report, KFK-1000 (1968).
8. G. D. James, Proc. Sym. on Neut. Stds., U.S. Natl. Bur. of Stds., Pub. NBS-SP 493 (1977).
9. A. B. Smith, P. Guenther, R. Larson, C. Nelson, P. Walker and J. F. Whalen, Nucl. Instr. and Methods, 50 277 (1967); see also P. Guenther, A. Smith and J. Whalen, Phys. Rev., C12 1797 (1975).
10. A. Smith, P. Guenther and R. Sjoblom, Nucl. Instr. and Methods, 140 397 (1977).
11. J. Hopkins and G. Breit, Nucl. Data, A9 137 (1971).
12. P. T. Guenther, Univ. of Ill. Thesis, Elastic and Inelastic Neutron Scattering from the Even Isotopes of Tungsten (1977).
13. A. Smith, R. Holt and J. Whalen, Neutron Scattering from  $^{12}\text{C}$  in the Few MeV Region, Argonne National Laboratory Report, ANL/NDM-43 (1978).
14. D. L. Smith, "A Spectrometer for the Investigation of Gamma Radiation Produced by Neutron-Induced Reactions," Argonne National Laboratory Report, ANL/NDM-12 (1975).

15. Clement et al. (1971), data as provided by the National Nuclear Data Center, Brookhaven National Laboratory.
16. P. A. Moldauer, Private Communication.
17. S. Raman, Nuclear Data Sheets for A=60, B2-5-41 (1968).
18. W. Voss, Private Communication, data available from Neutron Data Compilation Center, Saclay, France, CCDN (1978).
19. D. L. Smith, "Fast-Neutron Gamma-Ray Production from Elemental Iron:  $E_n \sim 2$  MeV," Argonne National Laboratory Report, ANL/NDM-20 (1976).
20. P. Guenther, A. Smith, D. Smith, J. Whalen and R. Howerton, "Measured and Evaluated Fast Neutron Cross Sections of Elemental Nickel," Argonne National Laboratory Report, ANL/NDM-11 (1975).
21. K. Tsukada, S. Tanaka, Y. Tomita and M. Maruyama, Nucl. Phys., A125 641 (1969).
22. P. Boschung, J. T. Lindow and E. F. Shrader, Nucl. Phys., A161 593 (1971).
23. W. Rodgers, E. Shrader and J. Lindlow, Chicago Operations Office Report, COO-1573 33 (1967).
24. V. Sluchaevskaia, ANL Trans. 168, Bull. Information Center for Nucl. Data, USSR (1964).
25. R. Day, Phys. Rev., 102 767 (1956).
26. V. Scherre, B. Allison and R. Faust, Phys. Rev., 96 386 (1954).
27. F. Perey, C. LeRigoleur and W. Kinney, Oak Ridge National Laboratory Reports, ORNL-4523 (1970) and ORNL-4807 (1974).
28. Evaluated Nuclear Data File - B(ENDF/B) Version-IV, National Nuclear Data Center, Brookhaven National Laboratory.
29. P. Hodgson, The Optical Model of Elastic Scattering, Oxford Press, London (1963).
30. W. Hauser and H. Feshbach, Phys. Rev., 87 366 (1952).
31. P. A. Moldauer, Phys. Rev., 171 1164 (1963); Phys. Rev., C11 426 (1978); and Private Communication.

32. H. Hofmann, J. Richert, J. Tepel and H. Weidenmüller, Ann. Phys. (NY), 90 403 (1975).
33. A. Gilbert and A. G. W. Cameron, Can. Jour. Phys., 43 1446 (1965).
34. ABAREX-1 and 2, Digital Computer Programs, P. A. Moldauer, to be published.
35. C. Engelbrecht and H. Fiedeldey, Ann. Phys., 42 262 (1967).
36. S. Cierjacks, Proc. of NEANDC Specials Meeting on Neutron Data of Structural Materials for Fast Reactors, Geel (1977).
37. P. H. Stelson and L. Grodzins, Nucl. Data, A1 21 (1965).
38. Coupled-Channels Digital Computer Program, JUPREX, P. A. Moldauer, Private Communication (1978).